Hindawi Publishing Corporation
Journal of Chemistry
Volume 2015, Article ID 749875, 11 pages
http://dx.doi.org/10.1155/2015/749875

Research Article

Effect of Zn/ZSM-5 and $FePO_4$ Catalysts on Cellulose Pyrolysis

Haian Xia, Xiaopei Yan, Siquan Xu, Li Yang, Yuejie Ge, Jing Wang, and Songlin Zuo

Jiangsu Key Lab of Biomass-Based Green Fuels and Chemicals, College of Chemical Engineering, Nanjing Forestry University, Nanjing 210037, China

Correspondence should be addressed to Haian Xia; haxia@dicp.ac.cn

Received 18 April 2015; Revised 25 June 2015; Accepted 25 June 2015

Academic Editor: Darren Sun

A series of Zn/ZSM-5 catalysts with different Zn contents and $FePO_4$ were used to pyrolyze cellulose to produce value added chemicals. The nature of these catalysts was characterized by ammonia-temperature programmed desorption (NH_3-TPD), IR spectroscopy of pyridine adsorption, and X-ray diffraction (XRD) techniques. Noncatalytic and catalytic pyrolytic behaviors of cellulose were studied by thermogravimetric (TG) technique. The pyrolytic liquid products, that is, the biooils, were analyzed by gas chromatography-mass spectrometry (GC-MS). The major components of the biooils are anhydrosugars such as levoglucosan (LGA), 1,6-anhydro-β-D-glucofuranose (AGF), levoglucosenone (LGO, 1,6-anhydro-3,4-dideoxy-β-D-pyranosen-2-one), and 1,4:3,6-dianhydro-α-*D*-glucopyranose (DGP), as well as furan derivatives, alcohols, and so forth. Zn/ZSM-5 samples with Brønsted and Lewis acid sites and the $FePO_4$ catalyst with Lewis acid sites were found to have a significant effect on the pyrolytic behaviors of cellulose and product distribution. These results show that Brønsted and Lewis acid sites modified remarkably components of the biooil, which could promote the production of furan compounds and LGO. On the basis of the findings, a model was proposed to describe the pyrolysis pathways of cellulose catalyzed by the solid acid catalysts.

1. Introduction

Woody biomass is being widely utilized as feedstocks for the production of the chemicals and transportation fuels. Cellulose, the most abundant terrestrial biopolymer, has been widely studied due to its potential to serve as a cheap resource for the production of chemicals such as anhydrosugars and furans derivatives through the pyrolysis process [1–7]. Catalytic pyrolysis is a high-effective thermal conversion pathway, which could be envisaged as a good method to increase productivity while decreasing undesired by-products, as well as upgrading the property of biooil [2, 8–15]. There are many value added compounds in biooil produced from cellulose pyrolysis such as levoglucosenone (LGO), which is the potential for useful chemicals [3, 5, 10].

The pyrolysis reactions are a very complex reaction including primary and secondary reactions, which are dependent upon the heating rate, the sample size, the type of catalyst, the reactor type, the reaction gas, and so forth [6]. Different pyrolytic mechanisms of cellulose have been proposed in past three decades, including the well-accepted Broido-Shafizadeh (B-S) model, the three-reaction model of Agarwal, Diebold's model, and so forth [8, 16, 17]. Bradbury et al. postulated that cellulose was subject to an initiation reaction to form an "active cellulose," which subsequently decomposed through two competitive first-order reactions [8]. Huber group's results showed that the majority of the char did not form from the "active cellulose" [6]. Instead, they assumed that the majority of the char was produced from the repolymerization of volatile anhydrosugar and fragmented species. LGO and DGP may further undergo fragmentation/retroaldol condensation, decarbonylation, dehydration, and decarboxylation to form small molecule products [6, 18]. However, more detailed mechanisms of cellulose pyrolysis are still under debate, especially for some secondary reaction mechanisms such as the conversion pathways of anhydrosugars.

It has been reported that solid oxides, super acids, inorganic proton acids, some inorganic salts, and so forth have a remarkable effect on the pyrolytic behaviors of cellulose

[1, 3, 4]. Rutkowski found that the $AlCl_3$ and $CuCl_2$ catalysts enhanced significantly the formation of LGO during the pyrolysis reaction of cellulose [4]. In addition, $CuCl_2$ catalyst was found to be more effective than $AlCl_3$ catalyst in the formation of LGO although $AlCl_3$ catalyst was a very powerful Lewis acid. The nanopowder metal oxides, such as SiO_2, TiO_2, MgO, and Al_2O_3-TiO_2, were reported to have significant influence on the pyrolytic behaviors of cellulose, especially for Al_2O_3-TiO_2, promoting the production of LGO and 1-hydroxy-3,6-dioxabicyclo[3.2.1]octan-2-one (LAC) [11]. Lu et al. and Wang et al. concluded that $ZnCl_2$ could promote the formation of furfural in the cellulose pyrolysis reaction [19, 20].

It was also revealed that zeolite catalysts have significant impacts on the biomass conversion and product selectivity [2, 11, 21, 22]. The zeolite catalysts containing transition metal oxides afford some special catalytic properties, such as olefin aromatization and oxidation-reduction, which the parent zeolite catalysts do not have, by incorporating some transition metal ions such as Ga, La, and Fe into the zeolite framework or channel [23–28]. The zeolite catalysts containing transition metal oxides have been widely used in petroleum refinery industry, N_2O direct decomposition, NO_x removal, and selective oxidation [26, 29]. Recently, these catalysts containing transition metal oxides have received increasing attention in the catalytic conversion of biomass. Huber et al. reported that bifunctional Ga/ZSM-5 catalysts exhibited the excellent catalytic performances in the conversion of furan to aromatic compounds because Ga species increased dramatically the rate of decarbonylation and olefin aromatization as compared to H-ZSM-5 catalyst [24]. Zn/ZSM-5 was found to have the excellent aromatization performances of furfural [30].

As described above, it is very important for a fundamental understanding of the role of Lewis and Brønsted acid sites during cellulose pyrolysis. The present study focuses on investigating the effect of Lewis and Brønsted acid sites on the pyrolytic behaviors of cellulose. For this purpose, we chose three types of catalysts, that is, Zn-ZSM-5 with Lewis and Brønsted acid sites, H-ZSM-5 mainly containing Brønsted acid sites, and $FePO_4$ catalyst with Lewis acid sites, to carry out the catalytic pyrolysis of cellulose. To the best of our knowledge, the use of Zn/ZSM-5 and $FePO_4$ catalysts in catalytic pyrolysis of cellulose has not been reported until now. A series of physicochemical techniques, including XRD, IR spectra of pyridine adsorption, and NH_3-TPR, were employed to characterize the nature of the catalysts.

2. Experimental

2.1. Preparation and Characterization of Catalysts. H-ZSM-5 catalyst with Si/Al ratio of 25 was purchased from Nankai University, China. Cellulose (cellulose powder, cotton linters, 435236-250G) and $FePO_4{\cdot}2H_2O$ catalysts were purchased from Sigma-Aldrich.

The Zn/ZSM-5 catalysts were prepared by incipient-wetness impregnation method. Typically, the H-ZSM-5 (Si/Al = 25) powder was impregnated with the solution of $Zn(NO_3)_2$. The mixtures were stirred at room temperature for 4 h and then dried in an oven at 120°C overnight. The dried powders were calcined at 550°C in flowing O_2 for 2 h. The three Zn/ZSM-5 catalysts were synthesized with the Zn loadings of 0.5, 1.3, and 2.7 wt% determined by inductively coupled plasma atomic emission spectroscopy (ICP-AES).

Ammonia-temperature programmed desorption (NH_3-TPD) measurements were conducted in a flow apparatus using a U-shaped quartz microreactor (4 mm internal diameter). The NH_3-TPD experiment was performed in the temperatures ranging from 50 to 800°C at a ramp rate of $10°C/min^{-1}$, and the desorbed ammonia was monitored by a gas chromatograph with a thermal conductivity detector (TCD).

IR spectra of pyridine adsorption were recorded on a Thermo Nicolet Nexus 470 spectrometer. Prior to measurement, a sample (20 mg) was pressed into a self-supported wafer and evacuated up to 10^{-2} Pa in an IR cell (attached to a vacuum line) at 450°C for 1.5 h. An IR background was recorded after the sample was cooled to room temperature. Subsequently, the wafer was exposed to pyridine vapor (equilibrium vapor at 0°C) for 20 min followed by outgassing for 30 min. The IR spectra were collected at different temperatures.

The BET surface areas were recorded on a ASAP2010 automated gas adsorption system. The samples were degassed at 300°C prior to analysis. The surface area of H-ZSM-5, 0.5 Zn/ZSM-5, and 2.6 Zn/ZSM-5 was 372.8, 374.3, and 368.9 m^2/g, respectively.

2.2. Pyrolysis of Cellulose. Thermogravimetric analysis (TGA) and derivative thermogravimetric (DTG) technique were performed using a TA Q5000 instrument. He gas was used as the sweep gas with a flow rate of 50 mL/min. Approximately 20 mg of cellulose or a mixture of cellulose with the catalyst was loaded in an alumina crucible.

A fixed-bed reactor was chosen for this study. A popular reactor like fluidized-bed was not selected because of the added complexity and variability of reactor parameter like mass and heat-transfer. In fact the added variability could actually shift from our focus on the impact of Lewis acid and Brønsted acid catalysts on cellulose pyrolytic behaviors. In this case, the fixed-bed reactor was helpful in ensuring reproducibility of results and was therefore fit for purpose. During a typical testing, a physical mixture consisting of catalyst and cellulose was prepared. Between 4 g and 6 g of ground material was loaded into a quartz-tube reactor and then ramped to reaction temperature in flowing N_2. An ice-water trap was used to collect the volatiles and heavy pyrolytic products. The yield of solid, that is, biochar, was determined gravimetrically, while the yield of biogas was calculated as remaining after quantification of the biooil and biochar. Finally, the water contents of the biooils were measured by means of the Karl Fisher titration according to the standard test procedure. The water contents of the biooils range from 35% to 45%.

2.3. GC-MS Analysis. The biooils were analyzed by Trace DSQ GC-MS with a HP-5 capillary column (30 m × 0.25 mm i.d., 0.25 μm film thickness). He gas was used as carrier gas with a constant flow of 20 mL/min and a 1 : 50 split ratio. The oven temperature was programmed from 60 to 260°C at

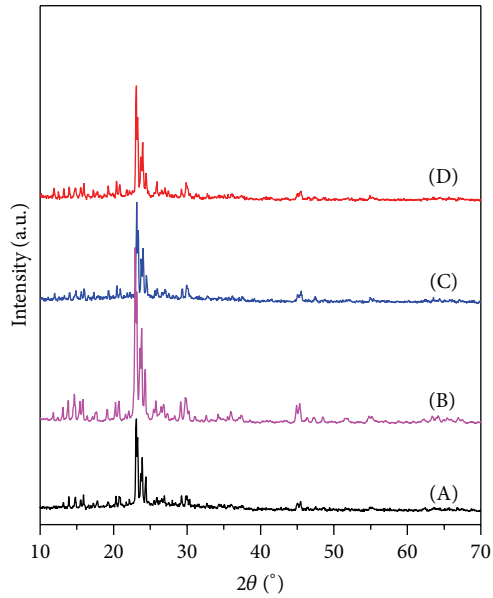

Figure 1: The XRD patterns of (A) H-ZSM-5, (B) 0.5 Zn/ZSM-5, (C) 1.3 Zn/ZSM-5, and (D) 2.7 Zn/ZSM-5.

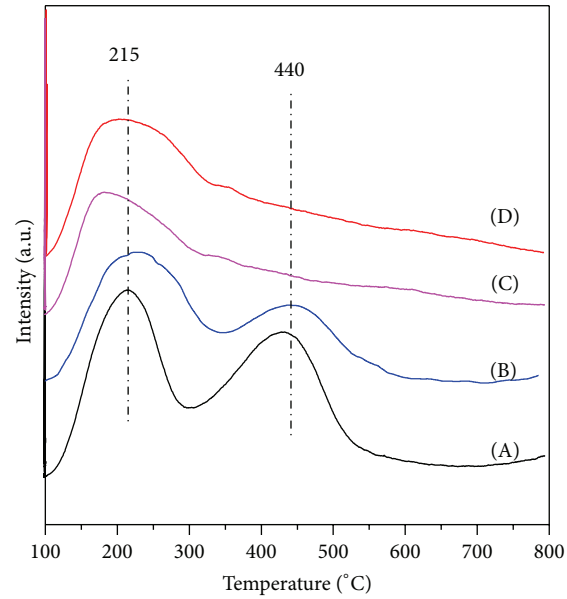

Figure 2: NH_3-TPD results of (A) H-ZSM-5, (B) 0.5 Zn/ZSM-5, (C) 1.3 Zn/ZSM-5, and (D) 2.7 Zn/ZSM-5.

a heating rate of 5°C/min and held at 260°C for 20 min. The injector was kept at a constant temperature of 300°C. A sample volume of 1 μL was injected. The total ion chromatography (TIC) results were applied for qualitative analysis. The identification of the peaks was based on computer matching of the mass spectra with the NIST library.

3. Results

3.1. Characterization of Catalyst. Figure 1 shows the XRD patterns of H-ZSM-5 (Si/Al = 25) and Zn/ZSM-5 with different Zn loadings. Several diffraction peaks of H-ZSM-5 are observed at 8°, 9°, 23°, 24°, 30°, and 35°, suggesting that the material is typical ZSM-5 zeolite structure. After the incorporation of Zn ions, no new diffraction peak appears, indicating that the introduction of Zn species did not destroy the zeolite structure and Zn species was highly dispersed over the H-ZSM-5 support.

To further investigate the evolution of acid sites after the incorporation of Zn ions, NH_3-TPD was carried out. Figure 2 presents the NH_3-TPD results of H-ZSM-5 and Zn/ZSM-5 catalysts with different Zn contents. Two desorption peaks around 215 and 440°C were observed for H-ZSM-5, which were assigned to weak acid sites and strong acid sites, respectively [31]. After loading Zn ions, the peaks at 215 and 440°C decreased for the three catalysts. Moreover, the peak at 440°C almost completely disappeared for 1.3 Zn/ZSM-5 and 2.6 Zn/ZSM-5. This indicates that the introduction of Zn ions resulted in the decrease of some strong acid sites; that is to say, the nature of acid sites would be changed.

To further evaluate the type of acid sites (Lewis and Brønsted) of H-ZSM-5 and Zn/ZSM-5, IR spectroscopy of pyridine adsorption was conducted. Figure 3 shows the IR spectra in the range of 1400–1600 cm^{-1} of pyridine adsorption on 0.5

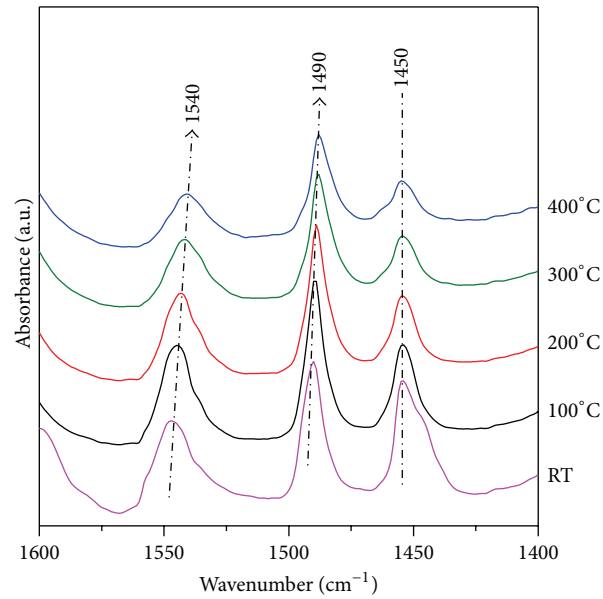

Figure 3: IR spectra of pyridine adsorption on 0.5 Zn/ZSM-5 at different desorption temperature.

Zn/ZSM-5 at different desorption temperatures. Three strong peaks are observed at 1450, 1490, and 1540 cm^{-1}, which are attributed to pyridine adsorbed on Lewis acid sites, Lewis and Brønsted acid sites, and Brønsted acid sites, respectively [31]. The Brønsted acid sites of the catalysts are derived from charge compensated hydrogen protons located at cationic ion-exchange sites of zeolite [31]. It is obvious that the three bands are relatively stable even at temperature greater than 400°C, which is consistent with the NH_3-TPD results. Figure 4 illustrates the IR spectra in the range of 1400–1600 cm^{-1} of pyridine adsorption on H-ZSM-5 and Zn/ZSM-5 catalysts

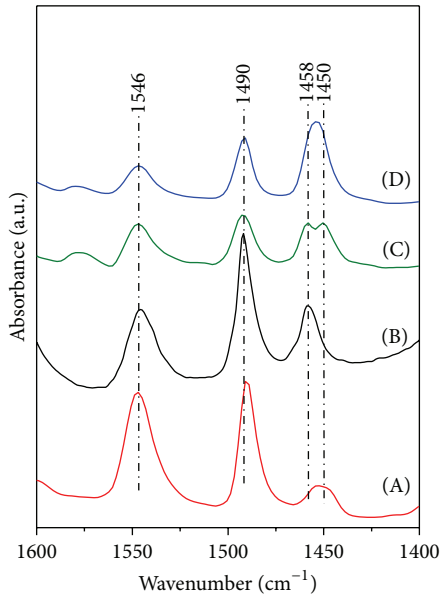

FIGURE 4: IR spectra of pyridine adsorption on (A) H-ZSM-5, (B) 0.5 Zn/ZSM-5, (C) 1.3 Zn/ZSM-5, and (D) 2.7 Zn/ZSM-5 at 200°C.

at 200°C. For H-ZSM-5, the band at 1450 cm^{-1} could be assigned to the Lewis acid sites derived from extra-framework Al species. A new band at 1458 cm^{-1} is also observed for the three Zn/ZSM-5 samples, showing that the introduction of Zn species forms new Lewis acid sites. The intensity of the band at 1546 cm^{-1}, assigned to Brønsted acid sites, decreases with increasing Zn loading. This means that part of ion-exchange H^+ sites of H-ZSM-5 were exchanged by Zn cations upon the introduction of Zn species, which is also evidenced by the NH_3-TPD results in which the peak area at 440°C decreases with increasing Zn content (Figure 2). To further illustrate the effect of incorporating Zn species on Brønsted and Lewis acid sites, the integral area ratios of Lewis acid sites to Brønsted acid sites were calculated. The L/B ratio is 0.14, 0.63, 1.16, and 1.97 for H-ZSM-5, 0.5 Zn/ZSM-5, 1.3 Zn/ZSM-5, and 2.7 Zn/ZSM-5, respectively. This clearly demonstrates that the introduction of Zn species increased the concentration of Lewis acid sites and formed new Lewis acid sites.

3.2. Catalytic Pyrolysis of Cellulose with Zn/ZSM-5 Catalysts. To study the impact of Zn/ZSM-5 on the pyrolytic behaviors of cellulose, TG method was employed. Figure 5(a) shows the TG curves of noncatalytic pyrolysis of cellulose and catalytic pyrolysis of cellulose with H-ZSM-5 and Zn/ZSM-5. There was an initial mass loss (approximately 10% of total weight) from 30°C and 170°C due to water desorption from feedstock. It was also observed that considerable mass loss occurred in the temperature range of 170–400°C and that thermal decomposition was essentially finished at 550°C. As the temperature was greater than 550°C, mass loss was less than 5%.

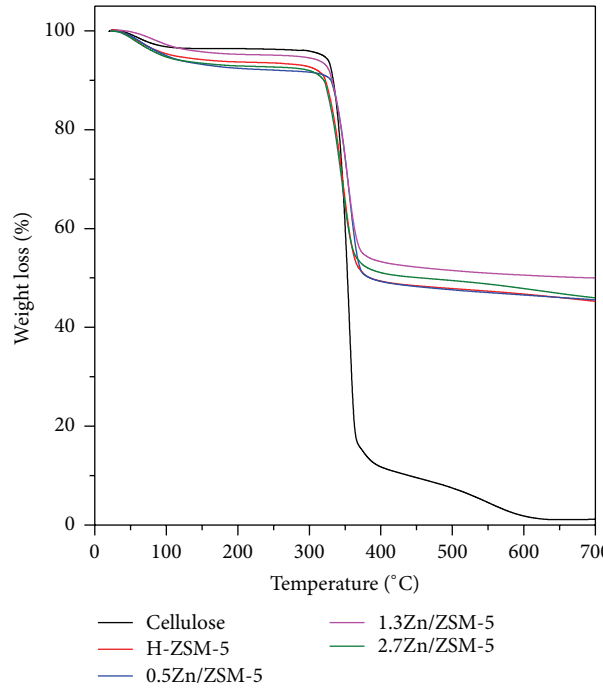

(a)

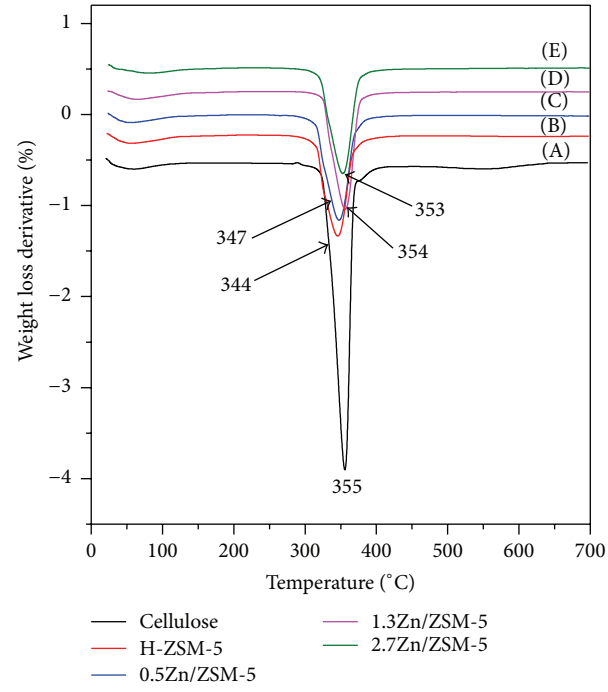

(b)

FIGURE 5: (a) TG and (b) DTG curves of (A) the noncatalytic pyrolysis of cellulose, (B) the catalytic pyrolysis of cellulose with H-ZSM-5, (C) the catalytic pyrolysis of cellulose with 0.5 Zn/ZSM-5, (D) the catalytic pyrolysis of cellulose with 1.3 Zn/ZSM-5, and (E) the catalytic pyrolysis of cellulose with 2.7 Zn/ZSM-5. The mass ratio of the catalyst to cellulose is equal to 1.

Table 1: The yield of biooil, biogas, and biochar obtained from cellulose pyrolysis at 400°C.

Catalyst	Reaction temperature (°C)	Yield of biooil (%)	Yield of biochar (%)	Yield of biogas (%)
—	400	52.1	26.3	21.7
H-ZSM-5	400	57.5	15.0	27.5
0.5 Zn/ZSM-5	400	57.0	19.8	23.2
1.3 Zn/ZSM-5	400	50.5	18.2	31.3
2.7 Zn/ZSM-5	400	45.2	26.8	28.0

Table 2: The effect of reaction temperature on the biooil components obtained from cellulose pyrolysis catalyzed by 0.5 Zn/ZSM-5 (peak area% in the MS).

Compound	350°C	400°C	450°C
Furfural	7.70	19.89	3.54
Butyrolactone	7.27	1.74	6.57
2-Furancarboxaldehyde, 5-methyl	1.80	3.89	1.48
Levoglucosenone (LGO)	0.93	6.21	4.01
1,4:3,6-Dianhydro-α-*D*-glucopyranose (DGP)	10.69	7.34	6.76
5-Hydroxymethylfurfural (5-HMF)	2.55	4.88	2.97
cis-1,2-Cyclehexanediol	1.70	1.08	1.13
Levoglucosan (LGA)	13.56	11.82	13.32
1,6-Anhydro-β-D-glucofuranose (AGF)	1.86	1.50	1.37

Figure 5(b) shows the DTG curves of the noncatalytic pyrolysis of cellulose and catalytic pyrolysis of cellulose with H-ZSM-5 and Zn/ZSM-5 with different Zn loadings. It can be seen that the maximum weight loss rate reached was at about 355°C for noncatalytic pyrolysis. Furthermore, the addition of H-ZSM-5 caused a shift of the maximum weight loss temperature to a lower temperature, demonstrating that the presence of acid sites could lower the pyrolytic temperature of cellulose, that is, promoting the cellulose pyrolysis.

Table 1 presents the yield of biooil, biochar, and biogas produced from the noncatalytic pyrolysis and catalytic pyrolysis of cellulose with Zn/ZSM-5 catalysts. As can be seen, the presence of H-ZSM-5 and 0.5 Zn/ZSM-5 resulted in an increase of the biooil yield accompanied by a decrease in the biochar production when compared to the noncatalytic pyrolysis of cellulose. However, with increasing Zn content, the presence of 1.3 Zn/ZSM-5 and 2.7 Zn/ZSM-5 catalysts increased the biogas yield and decreased the biooil yield as compared to the noncatalytic pyrolysis and catalytic pyrolysis of cellulose with H-ZSM-5 and 0.5 Zn/ZSM-5.

Table 2 shows the effect of reaction temperature on the biooil components obtained from cellulose pyrolysis catalyzed by the 0.5 Zn/ZSM-5 catalyst. The percentages of furan derivatives and LGO reached a maximum value as the temperature was 400°C. This result is in agreement with the work of Branca et al. in which the highest yield of furfural was achieved at 400°C during corncob pyrolysis catalyzed by acid catalysts [18].

Table 3 presents the component analysis of biooil derived from cellulose pyrolysis catalyzed by H-ZSM-5 and Zn/ZSM-5 catalysts. It should be noted that the obtained biooils contained several hundred compounds, but the table only gave some components with relatively high content. For catalytic pyrolysis of cellulose with Zn/ZSM-5 catalysts, the main constituents of biooil are anhydrosugars such as LGA, LGO, AGF, and DGP, furan derivatives, and alcohols. In addition, with increasing the Zn content, the percentage of furfural in the biooils produced from cellulose pyrolysis catalyzed by H-ZSM-5, 0.5 Zn/ZSM-5, 1.3 Zn/ZSM-5, and 2.7 Zn/ZSM-5 was 8.37, 19.89, 28.61, and 23.58%, respectively. It was also found that the addition of the acidic catalysts resulted in an increase in other furan derivatives besides furfural, implying that adding catalysts promoted considerably the formation of furan derivatives.

3.3. Catalytic Pyrolysis of Cellulose with $FePO_4$ Catalyst. Figure 6(a) exhibits the TG curves of noncatalytic pyrolysis of cellulose and catalytic pyrolysis of cellulose with different mass ratio of $FePO_4$ catalyst to cellulose. Similar to the pyrolysis of cellulose catalyzed by zeolite catalysts, there were mainly two weight loss regions: one was the temperature range from 30°C to 170°C and the other temperature range was from 170 to 550°C, which were attributed to the release of water and volatiles, respectively.

Figure 6(b) shows the DTG curves of the noncatalytic pyrolysis of cellulose and catalytic pyrolysis of cellulose with $FePO_4$. The addition of $FePO_4$ resulted in a shift of the maximum weight loss temperature at 355°C for noncatalytic pyrolysis to a lower temperature at 335°C as the mass ratio of $FePO_4$ to cellulose was equal to 1. The maximum mass loss temperatures were 335, 334, and 324°C as the mass ratio of $FePO_4$ to cellulose was 1, 2, and 4, respectively, demonstrating that the increase of the mass ratio of $FePO_4$ to cellulose shifted their pyrolysis temperatures to lower temperatures; that is, the presence of $FePO_4$ could promote considerably the pyrolysis of cellulose.

Table 4 lists the yield of biooil, biochar, and biogas produced from catalytic pyrolysis of cellulose with $FePO_4$ catalyst. The reaction temperature and the mass ratio of $FePO_4$ to cellulose had a significant effect on the yield of biogas, biooil, and biochar. With increasing the reaction temperature, a decrease in the biooil yield was accompanied by an increase in the biochar. As the mass ratio of $FePO_4$ to cellulose was equal to 2, the yield of biooil was up to 58.0%.

Table 3: The component analysis of the biooils derived from noncatalytic and catalytic pyrolysis of cellulose at 400°C (peak area% in the MS).

Compounds	Noncatalytic	H-ZSM-5	0.5 Zn/ZSM-5	1.3 Zn/ZSM-5	2.7 Zn/ZSM-5
Furfural	8.37	12.92	19.89	28.61	23.58
Furan, 2-propyl	—	0.76	0.90	5.24	3.93
Butyrolactone	—	—	1.74	1.07	2.83
5-Methyl-2-furanone	0.41	0.90	1.01	2.17	1.55
2-Furancarboxaldehyde, 5-methyl	1.87	2.75	3.89	6.67	6.43
Ethanone, 1-(2-furanyl)	1.03	1.93	1.32	2.75	1.86
2-Cyclopentene-1-one, 2-hydroxyl-3-methyl	2.31	1.47	1.05	2.32	1.63
Methyl 2-furnate	1.19	1.48	—	1.86	0.97
2,5-Dimethyl-4-hydroxy-3-furanone	—	—	2.29	1.20	0.80
Levoglucosenone (LGO)	3.26	21.40	6.21	4.30	0.47
1,4:3,6-Dianhydro-α-*D*-glucopyranose (DGP)	9.84	14.03	7.34	6.42	6.39
5-Hydroxymethylfurfural (5-HMF)	1.33	0.51	4.88	1.95	2.59
cis-1,2-Cyclehexanediol	1.85	1.42	1.08	1.08	2.17
Levoglucosan (LGA)	22.10	14.30	11.82	3.25	6.80
1,6-Anhydro-β-D-glucofuranose (AGF)	2.26	1.11	1.50	1.37	0.70

Table 4: The yield of biooil, biogas, and biochar produced from cellulose pyrolysis catalyzed by $FePO_4$ under different reaction conditions.

Reaction temperature (°C)	The mass ratio of catalyst to cellulose	Yield of biooil (%)	Yield of biochar (%)	Yield of biogas (%)
350	1	49.6	19.0	31.4
400	1	46.2	21.8	32.0
450	1	39.1	24.0	36.9
350	2	58.0	26.7	15.3
350	4	35.2	23.0	41.8

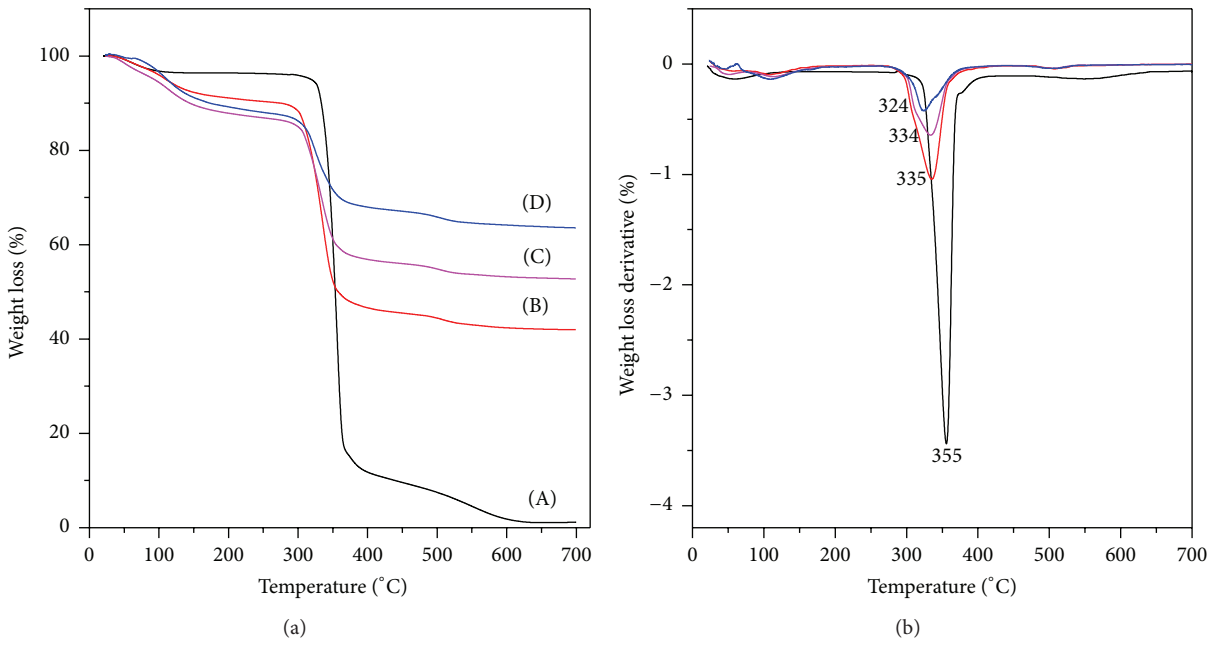

Figure 6: (a) TG and (b) DTG curves of (black) the noncatalytic pyrolysis of cellulose, (red) the catalytic pyrolysis of cellulose with $FePO_4$ ($m(FePO_4)/m$(cellulose) = 1), (magenta) the catalytic pyrolysis of cellulose with $FePO_4$ ($m(FePO_4)/m$(cellulose) = 2), and (blue) the catalytic pyrolysis of cellulose with $FePO_4$ ($m(FePO_4)/m$(cellulose) = 4).

Table 5: The component analysis of the biooils produced from noncatalytic and catalytic pyrolysis of cellulose with $FePO_4$ (peak area% in the MS).

Compound name	Noncat.[a]	$FePO_4$[b] 1 : 1-350	$FePO_4$[c] 1 : 1-400	$FePO_4$[d] 1 : 1-450	$FePO_4$[e] 2 : 1-350	$FePO_4$[f] 4 : 1-350
Furfural	12.67	23.55	15.32	17.28	20.29	25.12
Ethanone,1-(2-furanyl)-	0.48	1.05	1.00	1.14	0.73	0.37
2-Furancarboxaldehyde,5-methyl-	2.70	7.14	4.77	0.99	6.54	6.90
2-Cyclopenten-1-one,2-hydroxy-3-methyl-	2.03	0.79	4.25	2.19	4.47	0.36
Levoglucosenone (LGO)	17.43	32.75	17.87	19.98	23.98	16.31
3,5-Dihydroxy-2-methyl-4H-pyran-4-one (DHMP)	2.06	5.25	4.70	4.83	5.69	4.39
1,4:3,6-Dianhydro-α-*D*-glucopyranose (DGP)	12.59	8.36	9.94	8.84	6.61	5.98
5-Hydroxymethylfurfural	1.56	2.91	2.00	2.84	2.00	1.11
3,4-Anhydro-D-galactosan	0.48	0.60	0.27	—	0.46	0.63
cis-1,2-Cyclehexanediol	4.06	1.32	4.87	7.36	6.92	15.38
Levoglucosan (LGA)	22.78	4.87	11.98	4.63	4.55	3.58

[a]Noncatalytic pyrolysis of cellulose at 350°C.
[b]The reaction temperature at 350°C; the mass ratio of $FePO_4$ to cellulose is 1.
[c]The reaction temperature at 400°C; the mass ratio of $FePO_4$ to cellulose is 1.
[d]The reaction temperature at 450°C; the mass ratio of $FePO_4$ to cellulose is 1.
[e]The reaction temperature at 350°C; the mass ratio of $FePO_4$ to cellulose is 2.
[f]The reaction temperature at 350°C; the mass ratio of $FePO_4$ to cellulose is 4.

Table 5 presents the semiquantitative analysis of biooil components derived from the pyrolysis reaction of cellulose mixed with $FePO_4$ catalyst. The major constituents of biooil were anhydrosugars such as LGA, LGO, and DGP, as well as furan derivatives such as furfural and 2.5-dimethyl furan, alcohols, and 3,5-dihydroxyl-2-methyl-4H-pyran-4-one (DHMP). The production of DHMP is due to the dehydration reaction of LGA [32]. It is important to note that a new minor product, 3,4-anhydrogalactosan, was produced, which could be due to the dehydration of LGA. As shown in Table 5, the concentration of LGO in the biooils is 17.34, 32.75, 23.98, and 16.31% as the mass ratio of $FePO_4$ to cellulose is 0, 1, 2, and 4, respectively. The promotional effect was also observed for the production of furfural with increasing $FePO_4$ in the mixture.

4. Discussion

4.1. The Effect of Catalyst on the Pyrolysis of Cellulose. In the present work, main components of the biooils derived from noncatalytic and catalytic pyrolysis of cellulose were the anhydrosugars including LGO, DGP, AGF, and LGA, as well as its dehydration products such as furfural and 5-HMF (Tables 3 and 5). This result is in good agreement with the literature results [1, 5, 6, 10, 11]. It was reported that acidic catalysts, especially for Lewis acid catalysts such as $ZnCl_2$, were very effective for the conversion of anhydrosugars to furfural [1]. In addition, some other Lewis acid catalysts with the exception of Zn^{2+}, such as Fe^{3+} and Mg^{2+}, were found to facilitate the formation of furfural and other furan derivatives [18]. Our results also clearly showed that higher yields of furfural and other furan derivatives were obtained with the use of Zn/ZSM-5 than noncatalytic pyrolysis and H-ZSM-5 during the catalytic pyrolysis of cellulose (Table 3). In addition, Zn/ZSM-5 catalysts produced very small quantities of DGP when compared to noncatalytic pyrolysis of cellulose, suggesting that the catalysts were effective to catalyze the conversion of cellulose to furfural. In the present work, IR spectra of pyridine adsorption clearly demonstrated that new Lewis acid sites were generated upon incorporating Zn species to H-ZSM-5, which could be associated with a variety of Zn species. The presence of Zn/ZSM-5 was more effective than H-ZSM-5 in the decomposition of LGA, because the concentration of LGA in the biooil was lower with the use of Zn/ZSM-5 than H-ZSM-5. This showed that Brønsted and Lewis acid sites promoted the secondary reaction of LGA to produce LGO, furan derivatives, and so forth. The possible explanation is that Brønsted and Lewis acid sites enhanced the dehydration of the primary pyrolysis product.

It has been reported that Brønsted acid catalysts such as SO_4^{2-}/ZrO_2 and H_3PO_4 as well as Lewis acid catalysts such as $Fe_2(SO_4)_3$ favor the production of LGO during cellulose pyrolysis [3, 4, 10, 11]. In the present study, TG results showed that the maximum temperature of mass loss decreased with increasing the amount of $FePO_4$ during the pyrolysis reaction of cellulose, suggesting that $FePO_4$ enhanced effectively

the pyrolysis of cellulose. However, the yield of biogas increased with the increase of the $FePO_4$ amount in the pyrolysis reaction of cellulose. Thus, this result also showed that $FePO_4$ promoted the depolymerization and cracking reaction of the cellulose into noncondensable gases. Furthermore, $FePO_4$ also favored considerably the formation of LGO and furfural and decreased simultaneously the amount of LGA. It was showed that LGA did not break down when pyrolyzed alone [32]. However, we found that the addition of $FePO_4$ enhanced considerably the decomposition of LGA into the secondary reaction products. The possible reason is that the Lewis acid sites, that is, Fe^{3+} ions, promoted the dehydration reaction of LGA to LGO and furfural. The $FePO_4$ catalyst exhibited the higher furfural and LGO selectivity, while Zn/ZSM-5 catalysts had the higher furfural selectivity. The difference selectivities toward LGO and furfural for Zn/ZSM-5 and $FePO_4$ were observed because the Zn^{2+} and Fe^{3+} ions might have different acid strength and different coordination structure with LGA, thus leading to the different LGO selectivity. We found that $FePO_4$ could also facilitate the degradation of LGA to noncondensable gases besides LGO and furfural since the amount of LGA decreased with the increase of $FePO_4$ amount during the pyrolysis reaction. The possible interpretation is that $FePO_4$ enhanced the secondary catalytic cracking reactions of primary pyrolysis vapors.

4.2. The Effect of Acid Sites on the Pyrolytic Behaviors of Cellulose. As described above, Brønsted and Lewis acid sites played a vital role in the depolymerization of cellulose and its degradation products. TG results clearly showed that $FePO_4$ was more effective than H-ZSM-5 and Zn/ZSM-5 for the depolymerization of cellulose since the pyrolysis temperature was lower when $FePO_4$ was used to the catalyst. This can be explained by the fact that H-ZSM-5 and Zn/ZSM-5 micropore catalysts have small pore size and most acid sites are located into the zeolite channel. These properties lead to less contact with incoming pyrolytic substrates and therefore offer considerably less potential for cracking reactions to occur. However, it is more favorable for the contact between $FePO_4$ catalyst without regular micropore structure and cellulose as well as its pyrolytic products than those of H-ZSM-5 or Zn/ZSM-5 catalysts. Therefore, it is very reasonable that $FePO_4$ could decrease remarkably the pyrolytic temperature even if $FePO_4$ might have weak acidity.

Figure 7 depicts the effect of the L/B ratio on the percentages of furfural, LGO, DGP, and LGA of the biooil derived from catalytic pyrolysis of cellulose at 400°C. As can be seen, the percentage of furfural initially increased until the Zn content was 1.3 wt.% and then reduced with the increase of the L/B ratio. The percentages of LGO and DGP decreased with increasing the L/B ratio, suggesting the Lewis acid sites facilitated the decomposition of LGO and DGP into other small molecules such as furan derivatives and noncondensable gases containing CO and CO_2. LGO and DGP are considered as the secondary reaction product of LGA through a dehydration reaction, whereas LGO could be further dehydrated to furfural and other furan derivatives [1, 6, 10, 11]. The present work also showed that the Lewis acid sites, that is, highly dispersed Zn ions, facilitated the

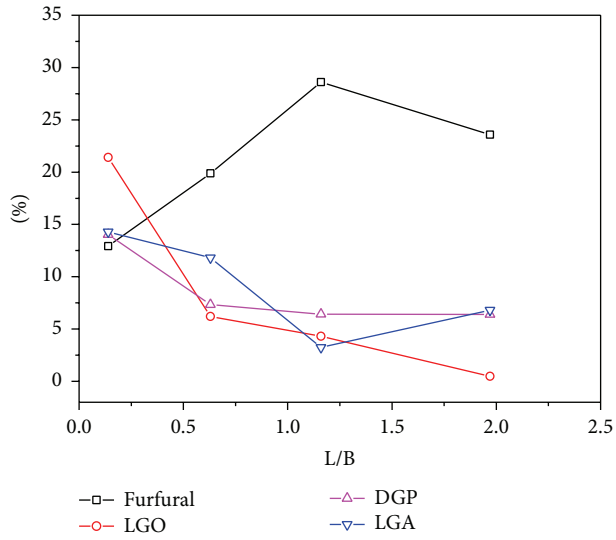

Figure 7: Effect of the L/B ratio of Zn/ZSM-5 on the percentage of (□) furfural, (○) LGO, (△) DGP, and (▽) LGA of the biooil derived from the catalytic pyrolysis of cellulose at 400°C.

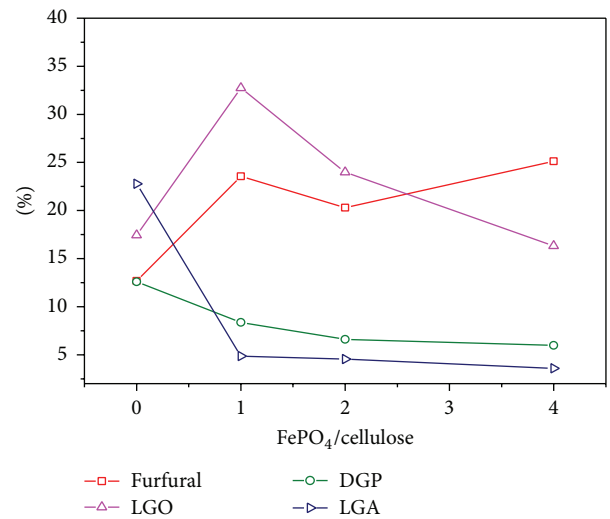

Figure 8: Influence of the mass ratio of $FePO_4$ to cellulose on the percentage of (□) furfural, (△) LGO, (○) DGP, and (▷) LGA of biooil produced from cellulose pyrolysis at 350°C.

production of furfural by promoting dehydration reactions of anhydrosugar such as LGO and DGP. It has been proposed that Zn/ZSM-5 catalysts have a high degree of heterogeneity of extraframework Zn species, including isolated Zn^{2+} cations, multinuclear oxygenated Zn clusters, and bulk ZnO aggregate [23, 31]. In good agreement with the results [23, 31], different Lewis acid sites were also formed in our Zn/ZSM-5 samples, which were evidenced by the two new IR bands of pyridine adsorption (Figure 4). These Zn/ZSM-5 catalysts with different Zn contents might exhibit various selectivity toward furan derivatives such as furfural and 5-methyl-2-furancarboxaldehyde, together with the different degradation activity of anhydrosugars during the catalytic pyrolysis of

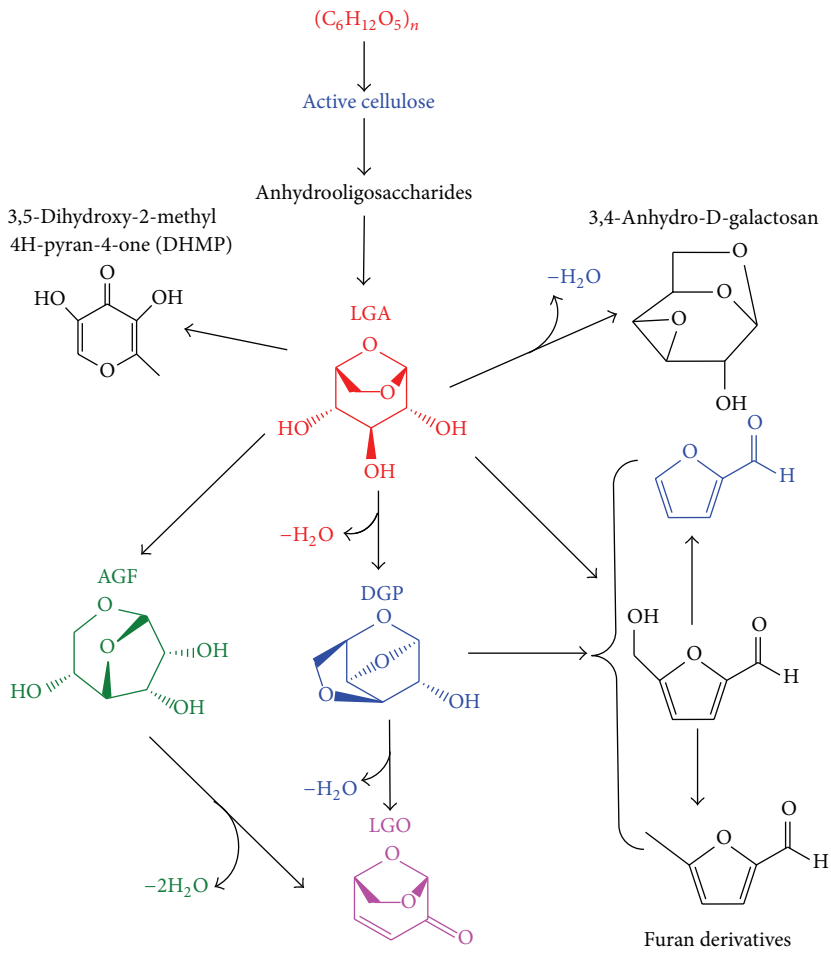

Figure 9: The possible conversion pathways of cellulose pyrolysis.

cellulose. One reason is that different properties of the Lewis acid sites would result in different catalytic performances during the pyrolysis of cellulose.

Figure 8 shows the influence of the mass ratio of $FePO_4$ to cellulose on the percentages of furfural, LGO, DGP, and LGA of the biooil produced from catalytic pyrolysis of cellulose at 350°C. It can be seen that the amounts of DGP and LGA decreased with increasing the mass ratio of $FePO_4$ to cellulose. As discussed above, LGA and DGP would be converted to furan derivatives and noncondensable gases, suggesting that $FePO_4$ enhanced effectively the decomposition of LGA and DGP and favored the formation of LGO. However, the amount of LGO decreased but the amount of furfural increased as the mass ratio of $FePO_4$ to cellulose increased to 4. This could be due to the fact that LGO was further converted as excess $FePO_4$ was used (Table 4).

4.3. The Possible Reaction Mechanism of Cellulose Pyrolysis. Figure 9 depicts the possible conversion pathways of cellulose pyrolysis. A formation pathway of LGA proceeds through active cellulose depolymerization to anhydrooligosaccharides followed by the cleavage of glycosidic bonds and then dehydration reaction. It is also possible that cellulose degradation during pyrolysis produces DGP and other anhydrosugars competitive to LGA formation [4]. LGO could be produced from LGA. The reaction pathway is that LGA could firstly undergo dehydration reaction to form DGP and then DGP was further dehydrated to LGO. A mechanism about the conversion of LGO to furfural was assumed by Matsuoka et al. [33]. They expected that the first step was hydrolysis via ring-opening of C_1-O_5 bond, evidenced by the presence of water vapor. Subsequently, there was the elimination of C_6 as formaldehyde before rearrangement into a five-member ring, which formed furfural upon elimination of water.

Furan derivatives are important secondary reaction products, which are formed through catalytic dehydration of anhydrosugars followed by rearrangement of rings [11, 20, 34]. 5-Methyl-furancarboxaldehyde was produced probably through the dehydration of 5-HMF followed by consecutive transfer hydrogen reaction, while furfural was possibly originated from the decarbonylation and dehydration reactions of 5-HMF. It is worth noting that a minor 2,5-furandicarboxaldehyde component was detected in biooil, which could undergo decarbonylation to furfural at high temperature. However, the formation mechanism of furan derivatives needs to be further investigated. In addition,

the amounts of furfural and 5-methyl-furancarboxaldehyde increased in the presence of $FePO_4$ and Zn/ZSM-5 catalysts during the pyrolysis reaction of cellulose, showing that the acid sites could favor effectively the production of the two compounds. Furthermore, a new product, that is, 3,4-anhydro-D-galactosan, was also detected in the cellulose pyrolysis reaction, which was most likely the dehydration product of LGA. However, it is also unclear for the production and transformation mechanism of the product during the pyrolysis process of cellulose.

5. Conclusions

Noncatalytic and catalytic pyrolysis of cellulose in the absence and presence of Brønsted and Lewis acid sites were carried out in order to investigate the effect of Brønsted and Lewis acid sites on the pyrolytic behaviors of cellulose and the nature of biooil. Zn/ZSM-5 samples with Brønsted and Lewis acid sites and $FePO_4$ with Lewis acid sites were employed to pyrolyze cellulose. The IR spectra of pyridine adsorption and NH_3-TPD results showed that Zn species was highly dispersed into the ZSM-5 support, and new Lewis acid sites were generated after the introduction of Zn species. TG results demonstrated that Zn/ZSM-5 and $FePO_4$ catalysts promoted significantly the pyrolysis of cellulose. The yields of furan derivatives were higher with the use of Zn/ZSM-5 and $FePO_4$ catalysts than those from noncatalytic pyrolysis of cellulose. It was found that Brønsted and Lewis acid sites promoted dramatically the secondary reaction and even changed the conversion pathways of anhydrosugars during the catalytic pyrolysis of cellulose. The highly dispersed Zn ions enhanced considerably the formation of furfural and furan derivatives, whereas $FePO_4$ promoted effectively the production of LGO and furfural.

Conflict of Interests

The authors declare that there is no conflict of interests regarding the publication of this paper.

Acknowledgments

This work was financially supported by the National Natural Science Foundation of China (Grant no. 31200445) and the Natural Science Foundation of Jiangsu province (Grant no. BK2012416). This work was also financially supported by Open Foundation of State Key Laboratory of Catalysis at Dalian Institute of Chemical Physics (N-12-09) and the Priority Academic Program Development of Jiangsu Higher Education Institutions (PAPD).

References

[1] Q. Lu, C.-Q. Dong, X.-M. Zhang, H.-Y. Tian, Y.-P. Yang, and X.-F. Zhu, "Selective fast pyrolysis of biomass impregnated with $ZnCl_2$ to produce furfural: analytical Py-GC/MS study," *Journal of Analytical and Applied Pyrolysis*, vol. 90, no. 2, pp. 204–212, 2011.

[2] D. J. Mihalcik, C. A. Mullen, and A. A. Boateng, "Screening acidic zeolites for catalytic fast pyrolysis of biomass and its components," *Journal of Analytical and Applied Pyrolysis*, vol. 92, no. 1, pp. 224–232, 2011.

[3] Z. Wang, Q. Lu, X.-F. Zhu, and Y. Zhang, "Catalytic fast pyrolysis of cellulose to prepare levoglucosenone using sulfated zirconia," *ChemSusChem*, vol. 4, no. 1, pp. 79–84, 2011.

[4] P. Rutkowski, "Catalytic effects of copper(II) chloride and aluminum chloride on the pyrolytic behavior of cellulose," *Journal of Analytical and Applied Pyrolysis*, vol. 98, pp. 86–97, 2012.

[5] P. Rutkowski, "Pyrolytic behavior of cellulose in presence of montmorillonite K10 as catalyst," *Journal of Analytical and Applied Pyrolysis*, vol. 98, pp. 115–122, 2012.

[6] Y.-C. Lin, J. Cho, G. A. Tompsett, P. R. Westmoreland, and G. W. Huber, "Kinetics and mechanism of cellulose pyrolysis," *Journal of Physical Chemistry C*, vol. 113, no. 46, pp. 20097–20107, 2009.

[7] D. A. Bulushev and J. R. H. Ross, "Catalysis for conversion of biomass to fuels via pyrolysis and gasification: a review," *Catalysis Today*, vol. 171, no. 1, pp. 1–13, 2011.

[8] A. G. W. Bradbury, Y. Sakai, and F. Shafizadeh, "A kinetic model for pyrolysis of cellulose," *Journal of Applied Polymer Science*, vol. 23, no. 11, pp. 3271–3280, 1979.

[9] J. Adam, M. Blazsó, E. Mészáros et al., "Pyrolysis of biomass in the presence of Al-MCM-41 type catalysts," *Fuel*, vol. 84, no. 12-13, pp. 1494–1502, 2005.

[10] G. Dobele, G. Rossinskaja, T. Dizhbite, G. Telysheva, D. Meier, and O. Faix, "Application of catalysts for obtaining 1,6-anhydrosaccharides from cellulose and wood by fast pyrolysis," *Journal of Analytical and Applied Pyrolysis*, vol. 74, no. 1-2, pp. 401–405, 2005.

[11] D. Fabbri, C. Torri, and V. Baravelli, "Effect of zeolites and nanopowder metal oxides on the distribution of chiral anhydrosugars evolved from pyrolysis of cellulose: an analytical study," *Journal of Analytical and Applied Pyrolysis*, vol. 80, no. 1, pp. 24–29, 2007.

[12] Q. Lu, W.-M. Xiong, W.-Z. Li, Q.-X. Guo, and X.-F. Zhu, "Catalytic pyrolysis of cellulose with sulfated metal oxides: a promising method for obtaining high yield of light furan compounds," *Bioresource Technology*, vol. 100, no. 20, pp. 4871–4876, 2009.

[13] A. M. Azeez, D. Meier, J. Odermatt, and T. Willner, "Effects of zeolites on volatile products of beech wood using analytical pyrolysis," *Journal of Analytical and Applied Pyrolysis*, vol. 91, no. 2, pp. 296–302, 2011.

[14] G. T. Neumann and J. C. Hicks, "Novel hierarchical cerium-incorporated MFI zeolite catalysts for the catalytic fast pyrolysis of lignocellulosic biomass," *ACS Catalysis*, vol. 2, no. 4, pp. 642–646, 2012.

[15] H. Zhang, R. Xiao, H. Huang, and G. Xiao, "Comparison of non-catalytic and catalytic fast pyrolysis of corncob in a fluidized bed reactor," *Bioresource Technology*, vol. 100, no. 3, pp. 1428–1434, 2009.

[16] A. C. Eliseo Ranzi, T. Faravelli, A. Frassoldati, G. Migliavacca, S. Pierucci, and S. Sommariva, "Chemical kinetics of biomass pyrolysis," *Energy & Fuels*, vol. 22, pp. 4292–4300, 2008.

[17] J. L. Banyasz, S. Li, J. L. Lyons-Hart, and K. H. Shafer, "Cellulose pyrolysis: the kinetics of hydroxyacetaldehyde evolution," *Journal of Analytical and Applied Pyrolysis*, vol. 57, no. 2, pp. 223–248, 2001.

[18] C. Branca, C. Di Blasi, and A. Galgano, "Catalyst screening for the production of furfural from corncob pyrolysis," *Energy and Fuels*, vol. 26, no. 3, pp. 1520–1530, 2012.

[19] S. Leng, X. Wang, Q. Cai, F. Ma, Y. Liu, and J. Wang, "Selective production of chemicals from biomass pyrolysis over metal chlorides supported on zeolite," *Bioresource Technology*, vol. 149, pp. 341–345, 2013.

[20] Q. Lu, Z. Wang, C.-Q. Dong et al., "Selective fast pyrolysis of biomass impregnated with $ZnCl_2$: furfural production together with acetic acid and activated carbon as by-products," *Journal of Analytical and Applied Pyrolysis*, vol. 91, no. 1, pp. 273–279, 2011.

[21] A. Campanella and M. P. Harold, "Fast pyrolysis of microalgae in a falling solids reactor: effects of process variables and zeolite catalysts," *Biomass and Bioenergy*, vol. 46, pp. 218–232, 2012.

[22] T. R. Carlson, G. A. Tompsett, W. C. Conner, and G. W. Huber, "Aromatic production from catalytic fast pyrolysis of biomass-derived feedstocks," *Topics in Catalysis*, vol. 52, no. 3, pp. 241–252, 2009.

[23] S. M. T. Almutairi, B. Mezari, P. C. M. M. Magusin, E. A. Pidko, and E. J. M. Hensen, "Structure and reactivity of Zn-Modified ZSM-5 zeolites: the importance of clustered cationic Zn complexes," *ACS Catalysis*, vol. 2, no. 1, pp. 71–83, 2012.

[24] Y.-T. Cheng, J. Jae, J. Shi, W. Fan, and G. W. Huber, "Production of renewable aromatic compounds by catalytic fast pyrolysis of lignocellulosic biomass with bifunctional Ga/ZSM-5 catalysts," *Angewandte Chemie—International Edition*, vol. 51, no. 6, pp. 1387–1390, 2012.

[25] H. Xia, K. Sun, Z. Feng, and C. Li, "Effect of water on active iron sites for N_2O decomposition over Fe/ZSM-5 catalyst," *The Journal of Physical Chemistry C*, vol. 115, no. 2, pp. 542–548, 2011.

[26] H. Xia, K. Sun, Z. Liu, Z. Feng, P. Ying, and C. Li, "The promotional effect of NO on N_2O decomposition over the bi-nuclear Fe sites in Fe/ZSM-5," *Journal of Catalysis*, vol. 270, no. 1, pp. 103–109, 2010.

[27] K. Frey, L. M. Lubango, M. S. Scurrell, and L. Guczi, "Light alkane aromatization over modified Zn-ZSM-5 catalysts: characterization of the catalysts by hydrogen/deuterium isotope exchange," *Reaction Kinetics, Mechanisms and Catalysis*, vol. 104, no. 2, pp. 303–309, 2011.

[28] W. Huang, F. Gong, M. Fan, Q. Zhai, C. Hong, and Q. Li, "Production of light olefins by catalytic conversion of lignocellulosic biomass with HZSM-5 zeolite impregnated with 6wt.% lanthanum," *Bioresource Technology*, vol. 121, pp. 248–255, 2012.

[29] Q. Zhu, B. L. Mojet, R. A. J. Janssen et al., "N_2O decomposition over Fe/ZSM-5: effect of high-temperature calcination and steaming," *Catalysis Letters*, vol. 81, no. 3-4, pp. 205–212, 2002.

[30] W.-L. Fanchiang and Y.-C. Lin, "Catalytic fast pyrolysis of furfural over H-ZSM-5 and Zn/H-ZSM-5 catalysts," *Applied Catalysis A: General*, vol. 419-420, pp. 102–110, 2012.

[31] L. Yu, S. Huang, S. Zhang et al., "Transformation of isobutyl alcohol to aromatics over zeolite-based catalysts," *ACS Catalysis*, vol. 2, no. 6, pp. 1203–1210, 2012.

[32] M. S. Mettler, A. D. Paulsen, D. G. Vlachos, and P. J. Dauenhauer, "Pyrolytic conversion of cellulose to fuels: levoglucosan deoxygenation via elimination and cyclization within molten biomass," *Energy & Environmental Science*, vol. 5, no. 7, pp. 7864–7868, 2012.

[33] S. Matsuoka, H. Kawamoto, and S. Saka, "Influence of hydroxyl group configuration on pyrolytic formation of 1,6-anhydrohexopyranoses from various hexoses: an experimental and theoretical study," *Journal of Analytical and Applied Pyrolysis*, vol. 103, pp. 300–306, 2013.

[34] J. Nakayama and A. Miyake, "Catalytic effect of copper(II) oxide on oxidation of cellulosic biomass," *Journal of Thermal Analysis and Calorimetry*, vol. 110, no. 1, pp. 321–327, 2012.